Redox Biology 68 (2023) 102958

Contents lists available at ScienceDirect

Redox Biology

journal homepage: www.elsevier.com/locate/redox

A role for the cystathionine-β-synthase /H_2S axis in astrocyte dysfunction in the aging brain

Anindya Dey [a], Pijush Kanti Pramanik [a], Shailendra Kumar Dhar Dwivedi [a,d], Fiifi Neizer-Ashun [c], Tamas Kiss [e,f], Abhrajit Ganguly [h], Heather Rice [g], Priyabrata Mukherjee [b,d], Chao Xu [i], Mohiuddin Ahmad [c], Anna Csiszar [e], Resham Bhattacharya [a,c,d,*]

[a] Department of Obstetrics and Gynecology, University of Oklahoma Health Sciences Center, Oklahoma City, OK, 73104, USA
[b] Department of Pathology, University of Oklahoma Health Sciences Center, Oklahoma City, OK, 73104, USA
[c] Department of Cell Biology, The University of Oklahoma Health Sciences Center, Oklahoma City, OK, USA
[d] Peggy and Charles Stephenson Cancer Center, University of Oklahoma Health Sciences Center, Oklahoma City, OK, 73104, USA
[e] Vascular Cognitive Impairment and Neurodegeneration Program, Oklahoma Center for Geroscience and Healthy Brain Aging, Department of Biochemistry and Molecular Biology, University of Oklahoma Health Sciences Center, Oklahoma City, OK, USA
[f] Pediatric Center, Semmelweis University, Budapest, Hungary
[g] Department of Biochemistry & Molecular Biology, Oklahoma Center for Geroscience & Healthy Brain Aging, University of Oklahoma Health Sciences Center, Oklahoma City, OK, USA
[h] Section of Neonatal-Perinatal Medicine, Department of Pediatrics, University of Oklahoma Health Sciences Center, Oklahoma City, OK, USA
[i] Department of Biostatistics and Epidemiology, Hudson College of Public Health, The University of Oklahoma Health Sciences Center, Oklahoma City, OK, USA

ARTICLE INFO

Keywords:
Astrocyte
Aging
Hydrogen sulfide
Oxidative stress
Protein persulfidation

ABSTRACT

Astrocytic dysfunction is central to age-related neurodegenerative diseases. However, the mechanisms leading to astrocytic dysfunction are not well understood. We identify that among the diverse cellular constituents of the brain, murine and human astrocytes are enriched in the expression of CBS. Depleting CBS in astrocytes causes mitochondrial dysfunction, increases the production of reactive oxygen species (ROS) and decreases cellular bioenergetics that can be partially rescued by exogenous H_2S supplementation or by re-expressing CBS. Conversely, the CBS/H_2S axis, associated protein persulfidation and proliferation are decreased in astrocytes upon oxidative stress which can be rescued by exogenous H_2S supplementation. Here we reveal that in the aging brain, the CBS/H_2S axis is downregulated leading to decreased protein persulfidation, together augmenting oxidative stress. Our findings uncover an important protective role of the CBS/H_2S axis in astrocytes that may be disrupted in the aged brain.

1. Introduction

Astrocytes, the most abundant glial cells in the brain, are crucial to the proper functioning of the central nervous system (CNS). Astrocytes perform various functions in maintaining homeostasis of ions [1], and transmitters [2], provide metabolites to neurons [3], modulate local blood flow [4] and support the blood-brain barrier. Impaired astrocytic function and elevated oxidative stress are hallmarks of brain aging that are also associated with neurodegenerative diseases, including Alzheimer's [5] and Parkinson's disease [6]. However, signaling mechanisms underlying astrocytic dysfunction and the elevation in oxidative stress in aging and age-related diseases are not well understood.

Hydrogen sulfide (H_2S) is a gasotransmitter synthesized endogenously through depersulfidation of cysteine by two pyridodoxyl 5′-phosphate (PLP)-dependent enzymes: cystathionine β-synthase (CBS), cystathionine γ-lyase (CSE) [7], and by the PLP-independent 3-mercaptopyruvate sulfurtransferase (3-MST) [8]. Importantly, amongst these enzymes, astrocytes from the human [9] mouse [10] and rat brain [11] tissues express CBS. CBS catalyzes the first and rate-limiting step in the transsulfuration pathway, condensing serine and homocysteine (Hcy) generating cystathionine, a precursor for glutathione (GSH) and H_2S [7]. More than 150 mutations have been reported in the CBS gene [12,13] and patients with CBS deficiency show a spectrum of disease severity involving the eye, skeletal, central nervous and the vascular systems

* Corresponding author. Department of Obstetrics and Gynecology Peggy and Charles Stephenson Cancer Center, OUHSC, 975 NE 10th Street, BRC-1409B, Oklahoma City, OK, 73104, USA.
E-mail address: Resham-Bhattacharya@ouhsc.edu (R. Bhattacharya).

https://doi.org/10.1016/j.redox.2023.102958
Received 17 August 2023; Received in revised form 3 November 2023; Accepted 3 November 2023
Available online 6 November 2023

[13]. Notably, 33-75% of patients have mild or moderate developmental delay and behavioral abnormalities [14]. However, the exact role for the CBS/H_2S axis in astrocytes has not been defined.

It is well known that oxidative stress increases with age. Prior studies have established an inverse relationship between oxidative stress and a decrease in protein persulfidation [15]. We and others have shown that H_2S mediated persulfidation (-SSH) of cysteine thiol (-SH) residues on proteins leads to enhanced stability or activity of respective proteins [13,15,16]. Conversely, molecular interventions that increased protein persulfidation increased *C. elegans* lifespan by counteracting oxidative stress [15]. Interestingly, several neurodegenerative diseases are associated with oxidative stress and with H_2S [16]. For example, in a rat model of Amyloid-β (Aβ) driven Alzheimer's disease (AD) pre-treatment with H_2S donor, ameliorated neuroinflammation and improved spatial learning and memory [17]. However, the status of the CBS/H_2S axis in the aging brain and its possible role in astrocytes is unknown.

Here, we report that the expression of CBS and associated levels of H_2S decrease in the aging brain, resulting in a decrease in the overall persulfidated proteins and a decrease in the GSH/GSSG ratio contributing to oxidative stress. Our results suggest that the CBS/H_2S axis plays an important protective role in astrocytes that may be disrupted in the aged brain.

2. Materials and methods

2.1. Animal, cell culture and reagents

Young (2-3 months) and aged (24-26 months) C57BL6 male mice were obtained from the National Institute of Aging (NIA) rodent colony. After perfusion with ice-cold PBS for 15-20 min, the brains were collected, and cortex samples were separately snap frozen in liquid nitrogen (IACUC protocol: 21-030-SEAHIL). Normal Human Astrocytes (NHA) (CC-2565) were purchased from Lonza (Basel, Switzerland) and cultured in complete astrocyte growth medium (AGM) containing an astrocyte growth medium Bullet kit (Lonza, CC-3186). Primary Human Brain Microvascular Endothelial Cells (ACBRI 376) were purchased from Cell Systems Corporation (CSC) (Kirkland, WA, USA) and cultured in CSC Complete Medium (4Z0-500, CSC). All experiments were performed between passages 3-6. Primary human neuronal lysates were purchased from Science Cell (Carlsbad, CA, USA). NaHS, P-(4-methoxyphenyl)-P-4-morpholinyl-phosphinodithioic acid (GYY4137), and DTT were obtained from Sigma-Aldrich (St. Louis, MO, USA).

2.2. SDS-PAGE, and immunoblotting

Tissue or cellular lysate was prepared in Radio-Immunoprecipitation assay (RIPA) buffer (Boston BioProducts, Ashland, MA, USA), and protein concentration was measured using the Bicinchoninic acid (BCA) Assay Kit (Pierce, 23225). Tissue or cell lysates were separated on 10 or 12% glycine SDS-PAGE gel and transferred onto polyvinylidene difluoride membrane (Bio-Rad) followed by blocking in 5% bovine serum albumin (BSA) in tris-buffered saline (TBS) (Boston Bioproducts) with 0.1% Tween 20 (TBST). Membranes were probed with the following primary antibodies; CBS (14782), CSE (19689), β-actin (4970), and HSP90 (4877) from Cell Signaling Technology, 3MST (MABS1171) from Sigma-Aldrich; and secondary antibodies conjugated with horseradish peroxidase immunoglobulin G rabbit and mouse from Sigma-Aldrich.

2.3. H_2S measurement

H_2S was measured according to our published protocol [13,18]. Briefly, each mice brain flash frozen tissue was homogenized in PBS (pH 7.4) and protein concentration estimated. Approximately 1 mg protein was then transferred directly into a tube containing zinc acetate (1% wt/vol, 187.5 μl) and NaOH (12%, 12.5 μL) to trap the H_2S for 20 min at room temperature. The reaction was terminated by adding 1 mL of H_2O (pH 12.8), 200 μL of N, N-dimethyl-p-phenylenediamine sulfate (20 mM in 7.2 M HCl), and 200 μL of $FeCl_3$ (30 mM in 1.2 M HCl). The mixture was incubated for 15 min, and 600 μL was added to a tube with 150 μL of trichloroacetic acid (10% wt/vol). The precipitated protein was removed by centrifugation at 10,000 g for 5 min, and absorbance at 670 nm of the resulting supernatant was determined. The H_2S concentration of each sample was calculated against a calibration curve of NaHS.

2.4. RNA isolation and analysis of gene expression by RT-qPCR

RNA extraction was performed using RNeasy Plus Mini kit, Qiagen (CA, USA) following the manufacturer's protocol. Complementary DNA (cDNA) was prepared using iScript cDNA Synthesis kit (Bio-Rad) and RT-qPCR was performed using iTaq SYBR Green (Bio-Rad) following suppliers' protocols. All primers were from Integrated DNA Technologies (IDT) (Coralville, IA, USA) as listed below. The comparative Ct method [13] was used to calculate the relative abundance of the mRNA and compared with that of 18*S* ribosomal RNA (rRNA).

CBS (forward, 5′- GTAGCTTACAGGGCCTTTC -3′; reverse, 5′-CTAACCAGGTCCCTGAGGAT -3′); 18*S* rRNA (forward, 5′-CTCAACACGGGAAACCTCAC-3′; reverse, 5′-CGCTCCACCAACTAAGAACG-3′).

2.5. GSH/GSSG ratio for determination of oxidative stress

Mice brain cortex tissue was homogenized in lysis buffer (Abcam, ab179835), and centrifuged at 13,000g for 15 min. Supernatant was deproteinized following manufacturer's instructions (Abcam, ab204708). Resultant supernatant was used to determine reduced GSH, total GSH and oxidized GSSG, which was calculated as per manufacturer's instructions (Abcam, ab138881).

2.6. In-gel detection of persulfidation by the dimedone switch method

The assay was performed as described previously [15]. Briefly, either 15-20 mg of tissue per sample or 90% confluent NHA cells from a 10-cm culture dish was homogenized in cold HEN lysis buffer (100 mM Hepes, 1 mM EDTA, 0.1 mM neocuproine, 1% SDS) containing 1% protease inhibitor with supplementation of 10 mM 4-chloro-7-nitrobenzofurazan (NBF-Cl) and incubated at 37 °C for 1 h, protected from light. Lysates were centrifuged once subjected to methanol/chloroform precipitation. Precipitated protein was dissolved in 50 mM Hepes (pH 7.4) with 2% SDS. Protein concentration was determined using a BCA Assay kit (Pierce, 23225) and adjusted to approximately 3 mg/ml. DAz-2:Cy-5 click mix at 50 μM was added to the samples and incubated at 37 °C for 45 min, protected from light. Another methanol/chloroform precipitation was performed to remove excess click mix. The protein pellet was dissolved in Hepes with 2% SDS, boiled in Laemmli buffer (BioRad) and resolved by SDS-PAGE. The gel was imaged on the ChemiDoc MP (BioRad) and Cy5 and 488 nm signal recorded. NBF-Cl reacts with all amino groups giving a characteristic fluorescence with excitation maximum at 488 nm (green) that serves as a measure of the total protein load. Persulfidated proteins are detected by the Cy5 signal. Gel was also stained with InstantBlue (ab119211) as an additional measure of total protein load.

2.7. Microscopy of mitochondrial morphology

Briefly, NHA were plated on 12 mm coverslips and transfected with 30 nM control siRNA (siCTL Sigma #SIC001), or CBS siRNA (siCBS, Sigma-Aldrich; SASI_Hs01_00214623) using Lipofectamine™ RNAiMAX (Invitrogen, Carlsbad, CA, USA). 48 h after transfection cells were treated with MitoTracker Red (100 nM) for 15 min at 37 °C, after three washes with PBS, the cells were fixed with 4% PFA and stained with DAPI. Images were collected by Zeiss Axio Observer. Z1 (Göttingen, Germany) and analyzed for elongated or punctate mitochondria.

2.8. Cell mito-stress analysis

Different parameters of mitochondrial respiration were measured using the 96-well XF analyzer and the XF cell mito stress kit (Seahorse Bioscience, MI, USA). Assays were performed as per the manufacturer's protocol. SiRNA transfected cells were plated onto the 96-well XF assay plate at a cell density of 5×10^4 cells per well in complete AGM media. Thirty minutes before the assay, the plates were washed with the XF assay medium. Oligomycin (2 μM), FCCP (0.5 μM) and a mix of Antimycin A and Rotenone (1 μM each) were added into the appropriate ports and oxygen consumption rate (OCR) or extracellular acidification rate (ECAR) was recorded.

2.9. Mitochondrial ROS generation

To monitor the mitochondrial ROS production in CBS and control siRNA transfected astrocytes, a superoxide indicator MitoSOX Red (Molecular Probes, M36008) was used [19]. Briefly, 48 h after siRNA transfection cells were incubated with 2.5 μM of MitoSOX Red for 10 min at 37 °C in the dark. Cells were washed with PBS, and acquired via FACSCelesta flow cytometer (Becton Dickinson, Franklin Lakes, NJ, USA) and analyzed by FlowJo software (version 10.8.1).

2.10. Proliferation assay

NHAs were seeded at a density of 5×10^3 cells per well in 96-well plates. For Fig. 5A, cells were treated with increasing concentrations of Hcy (Sigma-Aldrich) (0-500 μM) for 60 h. For Fig. 6E, cells were treated with or without Menadione (10 μM) and/or 0.5 mM GYY for a period of 60 h. Cellular proliferation was assessed using the CyQUANT Assay Kit (Invitrogen, C35011). Fluorescence was measured by excitation at 508 nm and emission at 527 nm using CLARIOstar (BMG Labtech, Ortenberg, Germany).

2.11. ATP assay

Briefly, NHA were transfected with either control or CBS siRNA for 72 h. The CBS silenced cells were treated with 1 mM GSH (Fig. 5B) or with 0.5 mM GYY (Fig. 5C) for the last 60 h. For Fig. 5D, CBS-HA plasmid was transfected using Lipofectamine 3000 (Thermo Scientific) in CBS silenced cells for the last 36 h. ATP levels were measured using the Cell Titer-Glo® Assay (Promega) and luminescence recorded using a plate reader CLARIOstar (BMG Labtech, Ortenberg, Germany).

2.12. Data analysis and statistics

Data are expressed as mean ± SD or SEM as stated in figure legends. Analysis of variance (ANOVA) was performed to compare the mean among three or more groups and Student's *t*-test was performed to compare the mean between two groups. Statistical significance was set at $P < 0.05$ using GraphPad Prism 6 software. For bulk RNA-Seq data, a simple linear regression analysis was performed, and the R^2, P value of F-test statistic of overall significance are reported. For single cell RNA-Seq data, statistical analysis was performed using the FindMarker function from Seurat workflow, "test.use" parameter was set to the default Wilcoxon Rank Sum test.

3. Results

3.1. The expression of CBS is lower in the aged brain

To determine if the expression of CBS correlates with age, we analyzed publicly available RNA-Seq data from the human brain tissue as reported by Zhang et al., [20]. We applied a simple linear regression analysis where the relative abundance of CBS measured in fragments per kilobase of exon per million fragments mapped (FPKM) was regressed onto the age of the patient. We found that the expression of CBS significantly declined with age in both the whole cortex ($R^2 = 0.98$; $P = 0.009$) and astrocyte ($R^2 = 0.57$; $P = 0.004$) samples isolated from the human brain (Fig. 1A). We next performed reverse transcription quantitative real time PCR (RT-qPCR) to determine expression of CBS from murine brain cortical tissues. Corroborating the human RNA-Seq data, the expression of CBS mRNA was significantly lower in the aged 24–26-month-old compared to the young 2–3-month-old tissues (Fig. 1B). To confirm these observations at the protein level we performed immunoblotting for the three H_2S producing enzymes, CBS, CSE and 3-MST. At first, we determined antibody specificity by employing the murine liver tissues that served as positive control. The liver tissues prominently expressed CBS, CSE and 3-MST, however, the murine brain cortical tissues only showed expression of CBS and 3-MST but no CSE (Supplementary Fig. S1 and Fig. 1C). Compared to CBS (~1.72 fold), an insignificant (~1.07 fold) decrease in the expression of 3-MST was observed in the young vs aged murine brain tissues (Fig. 1C and D). Furthermore, in contrast to CBS (Fig. 1A), no significant correlation was observed between the mRNA expression of CSE and the age of patients either from the whole cortex or from the isolated astrocytes (Supplementary Fig. S2). Collectively, these results strongly suggest that CBS is the key H_2S producing enzyme in the brain, and its expression decreases in an age-dependent manner.

3.2. Intracellular protein persulfidation decreases in the aged brain

Previously, we and others have shown that H_2S mediated protein persulfidation plays an important role in protein activity [13,15]. Since the expression of CBS decreased in the aged brain samples, we measured the level of endogenous H_2S from mice brain cortical tissues using a modified methylene blue assay [13]. A constraint of the methylene-blue assay is that it measures total sulfide and not H_2S alone which can lead to overestimation of H_2S concentrations. Despite the constraints, the methylene-blue assay is widely utilized for H_2S measurements in biological samples [17,21–23]. H_2S levels significantly decreased in the aged group compared to the young group of samples (Fig. 2A). Since H_2S contributes to protein persulfidation, we used the highly selective modified dimedone-switch method [15] to determine level of persulfidation in young versus aged mice brain cortical tissues. In this assay, Cy5, red signal represents persulfidated proteins and 488 nm, green signal represents total protein load. We observed that the ratio of the Cy5/488 fluorescence signal significantly decreased in the aged versus the young murine brain cortical tissue samples (Fig. 2B and C).

Prior studies have established that the ratio of reduced to oxidized glutathione (GSSG) can be used as a relative measure of oxidative stress [24], which we assessed from the murine brain cortical tissues by using a fluorometric detection kit from Abcam (methods). Compared to the young group the GSH/GSSG ratio was significantly decreased in the aged group (Fig. 2D). Together these results support the conclusion that murine aged brain tissues have increased oxidative stress that is associated with reduced overall protein persulfidation.

3.3. CBS is predominantly expressed in the brain astrocytes

To determine which cell types in the human brain expressed CBS, we analyzed publicly available RNA-Seq data reported by Zhang et al., [20]. Astrocytes from the human brain tissues showed the highest expression of CBS as compared to other cell types (Fig. 3A). Similarly, astrocytes from the murine brain tissues [25] showed a trend towards higher CBS expression as compared to other cell types (Supplementary Fig. S3). To compare expression at the protein level we performed immunoblotting for CBS from the primary human astrocytes, primary human neurons and from the primary human brain microvascular endothelial cells (BMECs). Corroborating RNA-Seq data, we observed highest expression of CBS in astrocytes followed by neurons, with very low expression in the BMECs (Fig. 3B). Interestingly, analysis of single-cell RNA-Seq data

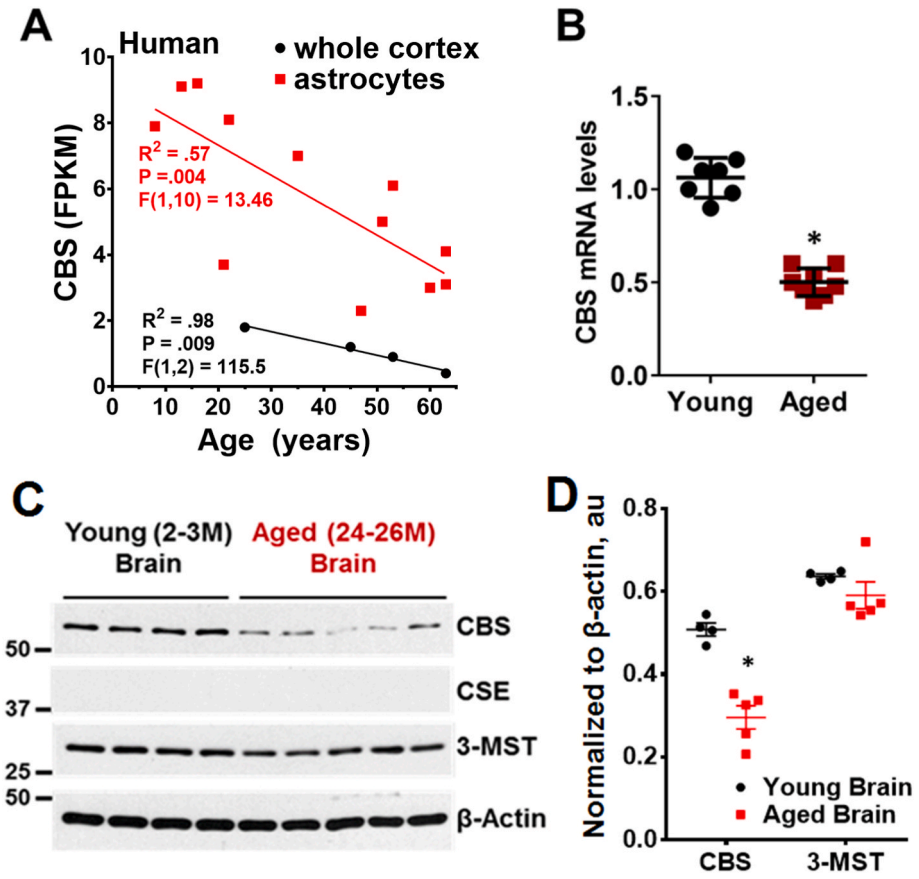

Fig. 1. The expression of CBS decreases with aging in the brain and in astrocytes. (A) Expression of CBS in human whole cortex and astrocyte samples as a function of age were derived from the publicly available RNA-Seq data [20]. Each data point represents an individual, 12 for astrocytes and 4 for the whole cortex. A simple linear regression analysis was performed, and the R^2, P value of F-test statistic of overall significance are reported. **(B)** mRNA expression of CBS in the young and aged mice brain cortex was determined by reverse transcription-quantitative polymerase chain reaction (RT-qPCR). 18S ribosomal RNA (rRNA) was used as an internal control. Error bar represents mean ± SD of 7 young and 8 aged mice performed in triplicate, *P < 0.05 when comparisons were made by Student's *t*-test. **(C)** Protein expression of CBS, CSE and 3-MST was determined from the young (2-3 month) and aged (24-26 month) mice brain cortex lysates by immunoblot. Each lane represents an individual mouse. β-Actin was used as loading control. **(D)** Densitometric analysis (arbitrary units, a.u. normalized with respect to β-actin) of immunoblots shown in C. Data represents mean ± SEM of 4 young and 5 aged brain samples, *P < 0.05 when statistical analysis was made by the Student's *t*-test. Fold change determined by the ratio of young/old. For CBS, 0.508/0.295 = 1.72; for 3-MST, 0.63/0.59 = 1.07.

from publicly available database [26] revealed that CBS was almost exclusively expressed by the murine brain astrocytes and although not statistically significant, expression was lower in the aged compared to the young group (Fig. 3C). These results indicate that CBS is predominantly expressed in the brain astrocytes.

3.4. Silencing CBS causes mitochondrial dysfunction in astrocytes

Changes in astrocytic mitochondrial function are intimately linked to age-related neurodegenerative diseases [27]. We previously showed that in human umbilical vein and in human aortic endothelial cells, CBS regulates mitochondrial dynamics [19]. Therefore, we next determined mitochondrial morphology and function in astrocytes following CBS downregulation with siRNA. Interestingly, in MitoTracker treated, control siRNA (siCTL) transfected astrocytes, ~80% of the cells presented with fused, filamentous mitochondria, whereas ~75% of the CBS-silenced cells showed mainly spherical, punctate mitochondrial morphology (Fig. 4A). To determine functionality, the mitochondrial oxygen consumption rate (OCR) and Extracellular Acidification Rate (ECAR) were measured (Fig. 4B and C) using the Seahorse XF-96 analyzer. Compared to the control cells, silencing CBS significantly decreased basal respiration by ~32% (Fig. 4D), relative ATP production by ~38% (Fig. 4E), FCCP-induced maximal respiration by ~48% (Fig. 4F) and the spare respiratory capacity by ~46% (Fig. 4G) indicating that mitochondrial function was impaired in the astrocytes. In the same assay, ECAR provides a measure of aerobic glycolysis. We observed that in the control cells, ECAR continuously increased as electron-transport chain inhibitors were added (Fig. 4C). However, the CBS silenced cells failed to increase their ECAR indicating inhibition of glycolysis (Fig. 4C). Given the mitochondrial dysfunction, we next measured ROS using the MitoSOX reagent. A significant, ~24% increase in mean fluorescence intensity (MFI) of MitoSOX Red in the CBS silenced group compared to the control (Fig. 4H) indicated enhanced ROS production. Together these results indicate that the CBS silenced astrocytes are compromised in their bioenergetics suggesting similar alterations in aging.

3.5. Impact of metabolites on astrocyte proliferation and bioenergetics

To determine if increased Hcy levels that are associated with inhibition of CBS [7] impacts proliferation, we treated the astrocytes with Hcy (0-500 μM) for 60 h and evaluated by the CyQuant assay. No significant change in astrocyte proliferation was observed (Fig. 5A). As shown above, mitochondrial dysfunction along with decreased levels of GSH and H_2S was observed upon CBS downregulation. Therefore, we used cellular ATP levels as a readout to determine any rescue by supplementation with GSH, H_2S or by re-expression of CBS. Compared to the control, a 29-35% decrease in relative ATP level was observed in CBS

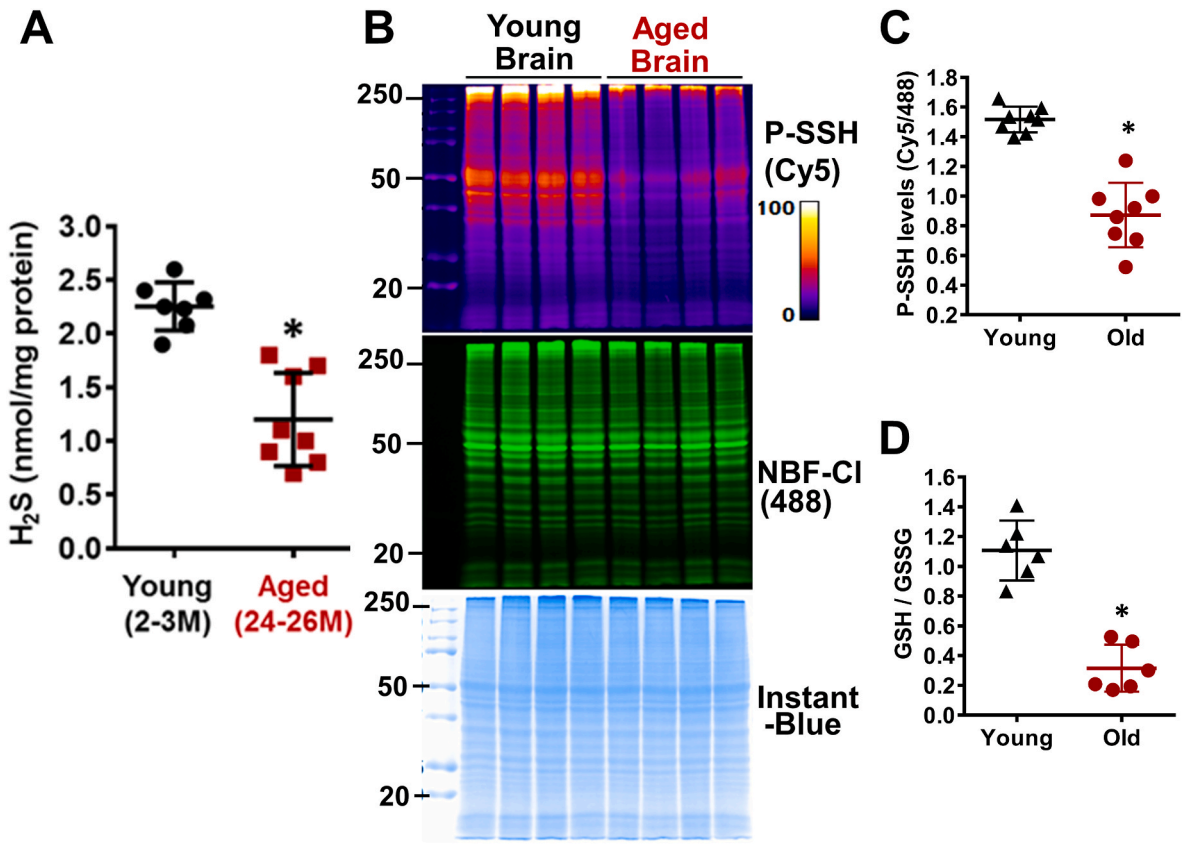

Fig. 2. H_2S levels and persulfidation (P-SSH) decrease while oxidative stress increases in the aged mice brain. (A) H_2S levels were determined by methylene blue assay. Error bar represents mean ± SD of 7 young and 8 aged mice performed in triplicate. *P < 0.05 when comparing by Student's *t*-test. **(B)** In-gel detection of changes in endogenous P-SSH levels in young (2-3 month) and aged (24-26 month) mice brain by dimedone switch assay. Young and aged mice brain cortex samples were lysed with supplementation of 10 mM NBF-Cl, and probed for P-SSH- labeling with DAz-2, followed by Cy5-alkyne using CuAAC. Fire pseudo-coloring was used to visually enhance the Cy5 signal. Green fluorescence corresponds to the total protein load (NBF-protein adducts). Gels were also stained with Instant blue to further confirm equal protein loading. **(C)** Ratio of Cy5/488 signals was used for the P-SSH quantification. Error bar represents mean ± SD of 8 young and 8 aged mice, *P < 0.05, Student's *t*-test. **(D)** Oxidative stress was measured in both young and aged mice brain cortex by a ratio of reduced glutathione (GSH): oxidized glutathione (GSSG) utilizing a fluorometric GSH/GSSG detection kit. Data represents mean ± SD of 6 young and 6 aged mice. *P < 0.05 when comparisons were made by Student's *t*-test.

silenced astrocytes (Fig. 5B and C). However, while supplementation with 1 mM GSH showed no rescue, supplementation with 0.5 mM GYY for 60 h rescued ATP levels by ~28% (Fig. 5B and C). Similarly, re-expression of CBS rescued ATP levels by ~31% in CBS-silenced astrocytes (Fig. 5D). Efficacy of CBS silencing and re-expression was confirmed at the protein level by immunoblotting (Fig. 5E). These results indicate that H_2S but not Hcy or GSH is an important consequential metabolite in the CBS pathway involved in astrocyte bioenergetics.

3.6. Oxidative stress impacts the CBS/H_2S axis

In the aged brain tissues, the increase in oxidative stress (Fig. 2D) is associated with a decrease in the expression of CBS (Fig. 1C). To probe this link further we treated the normal human astrocytes with hydrogen peroxide (H_2O_2), Menadione or with 2,3-dimethoxy-1,4-naphthoquinone (DMNQ), agents that have been previously shown to induce ROS [28]. Treatment with these ROS inducers prominently decreased the expression of CBS at 24 h (Fig. 6A) and significantly decreased H_2S levels in the cells (Fig. 6B). To determine the impact of decreased H_2S production on protein persulfidation we employed the modified dimedone-switch assay. We observed that the ratio of the Cy5/488 fluorescence signal prominently decreased in the Menadione and DMNQ treated cells compared to the control (Fig. 6C) indicating decreased overall protein persulfidation. To determine if H_2S supplementation could counteract the effect of ROS inducers, astrocytes were treated with Menadione in presence or absence of the H_2S donor, GYY for 24 h. Compared to the control, the ratio of the Cy5/488 fluorescence signal prominently decreased in the Menadione treated cells and increased in the GYY treated cells which served as positive control (Fig. 6D). However, compared to Menadione only, dual treatment with Menadione and GYY reversed overall protein persulfidation to near control levels (Fig. 6D). Next, to determine the impact of oxidative stress on astrocyte proliferation we used the CyQuant assay. Menadione or GYY treatment showed no effect at 12 h. However, after 36 h and 60 h, Menadione treatment significantly decreased astrocyte proliferation by ~27% and ~46% respectively (Fig. 6E). Compared to Menadione only, dual treatment with Menadione and GYY rescued astrocyte proliferation by ~18% and ~53% at 36 h and 60 h respectively (Fig. 6E). Together, these results indicate that there is a reciprocal relationship between oxidative stress and the CBS/H_2S axis. On the one hand, the CBS/H_2S axis by supporting mitochondrial bioenergetics protects astrocytes from oxidative stress, while, on the other hand, oxidative stress downregulates the CBS/H_2S axis in the aged brain leading to astrocyte dysfunction.

4. Discussion

Here we report an important reciprocal connection between the CBS/H_2S axis and oxidative stress in the aging brain, specifically in the astrocytes. Earlier we characterized the expression of CBS in different tissues and observed moderate to strong staining of CBS in endothelial

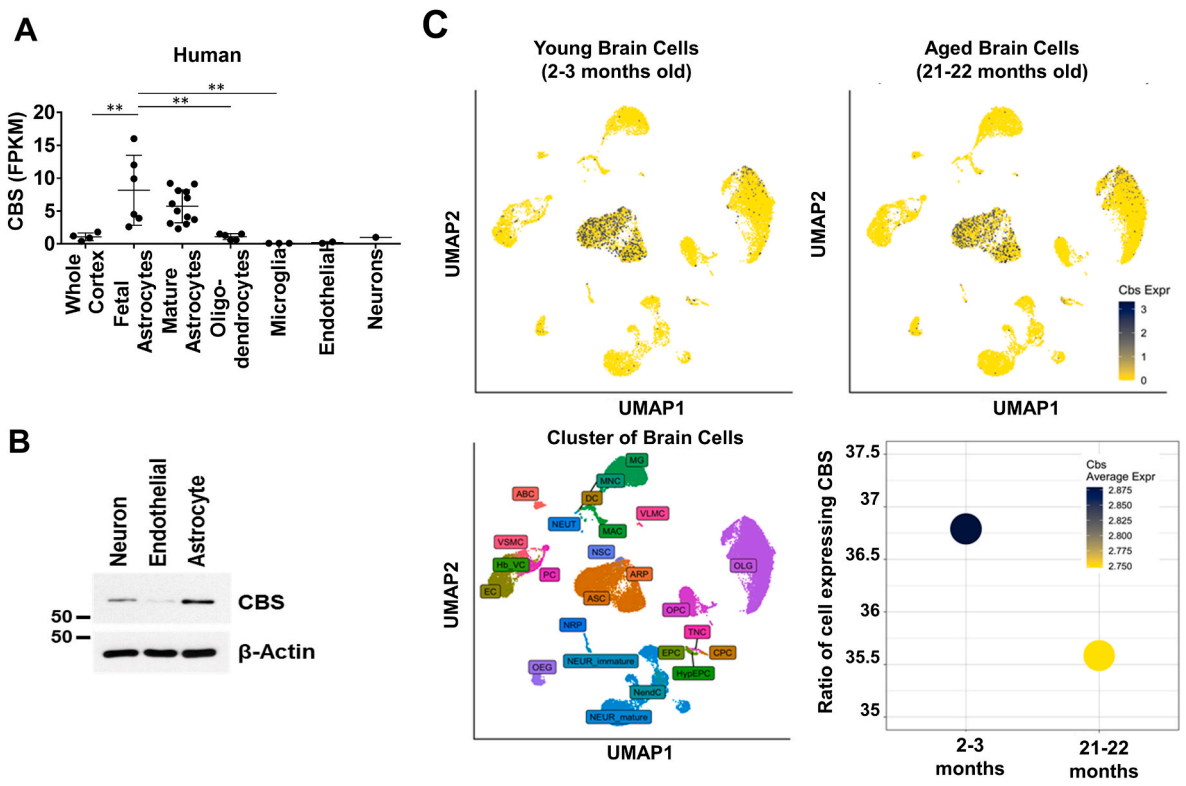

Fig. 3. Expression of CBS in different brain cell types and during aging. (A) Bulk cell expression of CBS in various cell types isolated from human brain were analyzed from the publicly available RNA-Seq data [20]. Each data point represents an individual, whole cortex, n = 4; fetal astrocytes, n = 6; mature astrocytes, n = 12; oligodendrocytes, n = 5; microglia, n = 3, endothelial, n = 2 and neurons, n = 1. Data represent mean ± SD. **P < 0.01 when Tukey's multiple comparisons were made by one-way ANOVA. The ANOVA table resulted in F(5, 26) = 7.083, p value = 0.0003. **(B)** Expression of CBS was determined from the human neurons, brain ECs and astrocytes by immunoblot. β-Actin was used as loading control. **(C)** Single cell expression of CBS in brain cells isolated from 2 to 3 months old and 21-22 months old mice were analyzed from the publicly available 10X Genomic single cell RNA sequencing data [26]. The data originated from 8 young (2–3 months) and 8 old (21–23 months) mice, from these animals 3327 young and 3420 old astrocytes were isolated and analyzed. Statistical comparison was performed using the FindMarker function from Seurat workflow, "test.use" parameter was set to the default Wilcoxon Rank Sum test. Result: p_val: 0.2330927; avg_log2FC: -0.05001576, p_val_adj = 1. MG: microglia; OLG: oligodendrocyte; EC: endothelial cells; ASC: Astrocytes; OPC: Oligodendrocyte progenitor cells; OEG: Olfactory ensheathing glia; NEURmat: mature neurons.

cells (ECs) of the normal ovary, granulosa cell tumors, normal colon, and lung adenocarcinoma. However, CBS was undetected in ECs of the normal liver, albeit a strong expression in hepatocytes [29] suggesting that endothelial beds from different tissues may show context specific expression of CBS. Here, we found that compared to the neurons and BMECs, the expression of CBS was strikingly enriched in the brain astrocytes as evidenced by the RNA-Seq and cellular protein level results.

One hallmark of aging and associated neurodegenerative diseases is a progressive increase in oxidative stress [30]. Prior reports from our and other groups, demonstrated increased oxidative stress upon depleting CBS in endothelial and in adipose-derived mesenchymal stem cells respectively [19,31]. Here, we found that both the mRNA and protein level expression of CBS but not CSE decreased in the aging brain tissues. According to reports, CSE is predominantly expressed in the murine kidney and liver tissues, with minimal expression in the brain [32], which corroborates our findings. Consequently, H_2S levels, associated protein persulfidation and the GSH/GSSG ratio decreased indicating enhanced oxidative stress. Zivanovic et al., reported that H_2S-mediated protein persulfidation prevents irreversible cysteine hyperoxidation preserving protein function and extending the lifespan of *C.elegans* [15]. Consistent with prior reports, our results suggest that there is an inverse relationship between the CBS/H_2S axis, associated persulfidation and oxidative stress that prevails in the aging brain.

Another hallmark of aging and associated neurodegenerative diseases is astrocytic dysfunction [33,34]. Depleting CBS in human astrocytes, altered mitochondrial morphology and compromised mitochondrial function that was associated with an increase in mitochondrial ROS and decreased ATP production. Interestingly, astrocytes rely heavily on glycolysis to meet local energy demands, however, they are also responsible for 20% of the brain's total oxygen consumption [27]. Strikingly, while the control cells were able to switch to glycolysis upon treatment with mitochondrial electron-transport chain inhibitors, the CBS depleted cells were unable to do so indicating that cellular bioenergetics was compromised suggesting similar alterations in aging. Interestingly, in CBS silenced astrocytes relative ATP level could be rescued by H_2S donors. These results are consistent with our prior reports where we showed that silencing CBS in human umbilical vein and in human aortic endothelial cells (HUVEC/HAOEC) caused mitochondrial dysfunction and enhanced receptor-mediated mitophagy that could be rescued by treatment with H_2S donors [19]. Mechanistically, important cellular persulfidation targets of H_2S have been described that could explain the bioenergetic phenotypes observed in the CBS depleted astrocytes. The mitochondrial inner membrane protein ATP synthase (F1F0 ATP synthase/Complex V) is persulfidated at cysteine residues 244 and 294. Mutation of these residues significantly decreases synthase activity and ATP output [35]. The prominent glycolytic enzyme, Glyceraldehyde-3-phosphate dehydrogenase (GAPDH), is persulfidated at cysteine residue 150 and mutation of this residue decreases activity [36]. Disruption of more than one signaling axis; a) mitochondrial dysfunction that can generate ROS, b) decreased cystathionine levels, a precursor for glutathione and/or c) decreased Nrf-2/Keap-1 antioxidant signaling because Keap-1 is a persulfidation target [37], may lead to oxidative stress that is observed in the CBS depleted astrocytes.

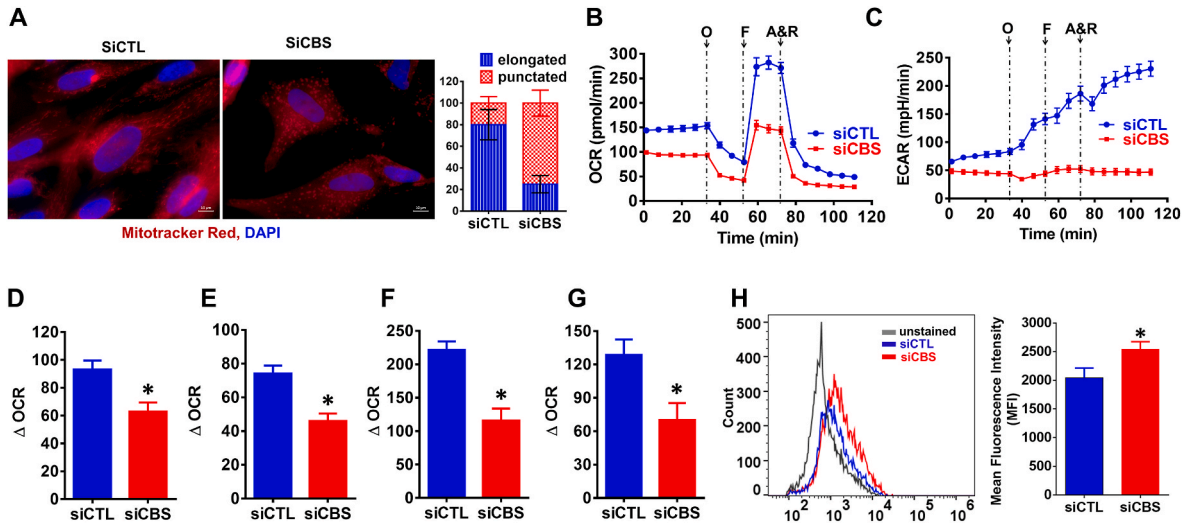

Fig. 4. Inhibition of CBS alters mitochondrial morphology and causes mitochondrial dysfunction in astrocytes. (A) Normal human astrocytes (NHA) were transfected with either scrambled (siCTL) or siCBS for 48 h. Mitochondrial morphology was determined by immunofluorescence utilizing the Mitotracker Red CMXRos. Each image is the representation of 3 independent experiments performed in triplicate, scale bar represents 10 μm. Approximately 200 cells from each treatment group from different fields were monitored and represented as with percent elongated or with percent punctated mitochondria. Data are the mean ± SD of atleast three independent experiments. *P < 0.05 when comparisons were made by Student's *t*-test. **(B, C)** Oxygen consumption rate (OCR) and Extracellular Acidification Rate (ECAR) were measured using the Seahorse XF-96 analyzer. NHA were transfected for 48 h with either scrambled (siCTL) or siCBS, and the OCR was measured. An XF trace representing mean ± SEM from 20 or more technical replicates per group is shown. Cells were sequentially treated with 2 μM Oligomycin (O), 0.5 μM FCCP (F) and 1 μM each of Antimycin + Rotenone (A&R) at indicated time points. Changes in OCR (Δ OCR) during **(D)** Basal respiration (before oligomycin), **(E)** ATP production (after oligomycin treatment), **(F)** FCCP-stimulated response (maximal respiratory capacity) and, **(G)** spare respiratory capacity (a measure of the ability of the cell to respond to increased energy demand or under stress) were derived from the XF trace of 2 independent experiments, represented as mean ± SEM from atleast 20 replicates per group. *P < 0.05 when comparisons were made by Student's *t*-test. **(H)** NHA were transfected for 48 h with either siCTL or siCBS, stained with MitoSOX Red and the mitochondrial ROS levels were measured using flowcytometry. Representative histogram of MitoSOX Red fluorescence intensity is shown, bar graph represents mean ± SD of mean fluorescence intensity (MFI) from three independent experiments,*P <0.05 by Student's t-test.

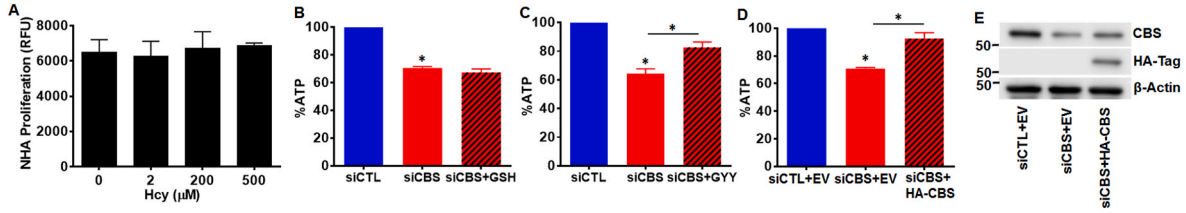

Fig. 5. The effect of metabolites on astrocyte proliferation and bioenergetics. (A) NHA were treated with Hcy (0-500 μM) for 60 h, and proliferation evaluated using the CyQUANT Assay. Data are the mean ± SEM of three independent experiments. (**B**) NHA were transfected with either siCTL or siCBS for 72 h and treated with 1 mM GSH for the last 60 h. ATP levels were evaluated using the CellTiter-Glo assay and control set at a 100%. Bar graph represents mean ± SEM from three independent experiments, *P <0.05 (Student's t-test) **(C)** NHA were transfected with either siCTL or siCBS for 72 h and treated with 0.5 mM GYY for the last 60 h. ATP levels were evaluated using the CellTiter-Glo Assay and control set at a 100%. Bar graph represents mean ± SEM from three independent experiments, *P <0.05 by Student's t-test. **(D)** Experiments similarly performed as in B and C, except HA-tagged CBS expressed [44] for the last 36 h. Data represents mean ± SEM from three independent experiments, *P <0.05 (Student's t-test). **(E)** Immunoblotting of lysates derived from experimental setup as in D.

Because we observed decreased expression of CBS in the aged brain tissues where systemic oxidative stress is multifactorial, we determined and found that chemically induced oxidative stress also decreased the expression of CBS, levels of H_2S, protein persulfidation and proliferation of astrocytes. The expression of CBS is regulated at the transcript level by the transcription factor, SP1 [38,39] and at the protein level by S-Adenosylmethionine (SAM) [40]. Notably, both factors are responsive to and may be altered upon oxidative stress [41] which could explain the observed decrease in the expression of CBS. Importantly, H_2S supplementation rescued oxidant-mediated decrease in astrocyte proliferation underscoring the importance of the CBS/H_2S axis in maintaining the health, function and redox balance in astrocytes, the most abundant brain cells.

We demonstrated that in the aged brain tissues, CBS was downregulated concurrent with decreased protein persulfidation and increased oxidant stress. Interestingly, recent studies have reported increase in plasma sulfide levels in Alzheimer's disease (AD) patients and correlated with cognition and microvascular disease [42,43]. The authors further discussed that elevated plasma polysulfides could be due to a compensatory pathway to restore normal neuronal homeostasis due to oxidative stress. Hence, the H_2S/persulfidation axis may have a tissue context dependent role that may be different in the normal aging brain versus in neurodegenerative diseases warranting further investigation.

5. Conclusion

In conclusion, the CBS/H_2S axis is downregulated in the aged brain which enhances oxidative stress by reducing overall protein persulfidation and causes mitochondrial dysfunction, ultimately impacting astrocyte health and proliferation. Thus, the CBS/H_2S axis plays an important protective role in maintaining astrocyte health, and its disruption may contribute to some of the age-related changes observed

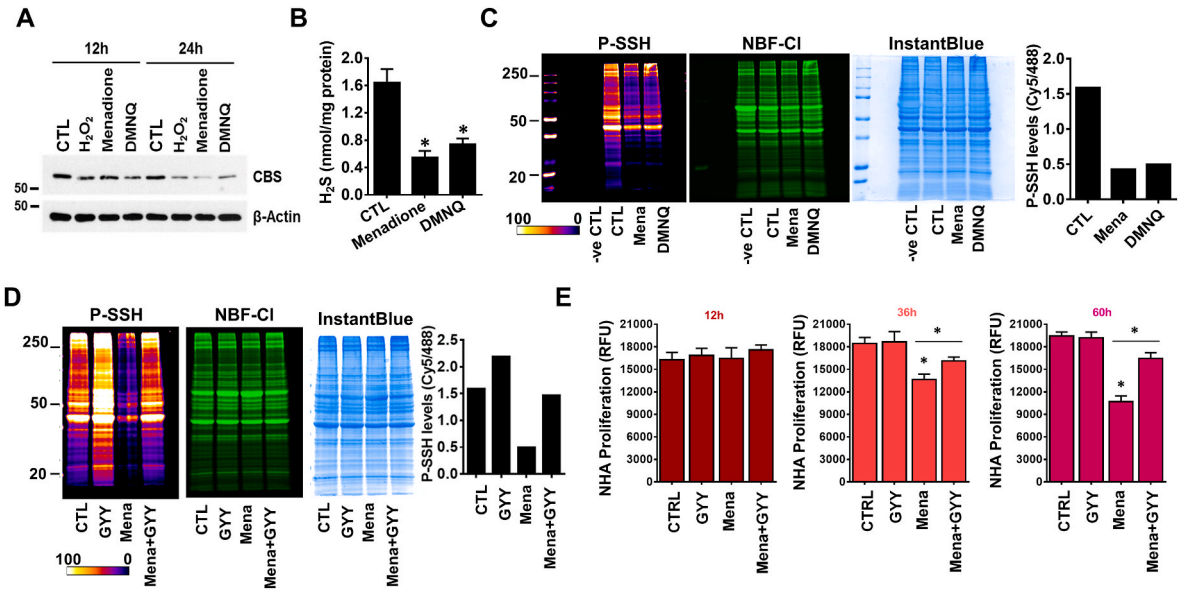

Fig. 6. Oxidative stress reduces expression of CBS and impairs persulfidation in human brain astrocytes. (A) NHA were treated with various ROS inducers: Menadione (10 μM), DMNQ (10 μM) and H_2O_2 (10 μM) for 24 h and expression of CBS was determined at 12- and 24 h time point. β-Actin was used as loading control. **(B)** H_2S levels were determined after 24 h of treatment utilizing methylene blue assay. Data represent mean ± SD of three independent experiments performed in triplicate, (*P < 0.05, one-way ANOVA). **(C)** The effect of oxidative stress on P-SSH levels in primary NHA. NHA were treated with or without Menadione (10 μM), DMNQ (10 μM) for 24 h and P-SSH levels were determined by dimedone switch assay. Negative control is the control group which was not probed for P-SSH-labeling with DAz-2, or Cy5-alkyne using CuAAC. **(D)** The impact of exogenous hydrogen sulfide supplementation was determined during induced oxidative stress. NHA were exposed to Menadione (10 μM) in the presence or absence of 0.5 mM of small-molecule slow-release H_2S generator, GYY4137 (GYY) for 24 h and P-SSH levels were determined by dimedone switch assay. **(E)** NHA were exposed to Menadione (10 μM) in the presence or absence of 0.5 mM GYY for 60 h, and cellular proliferation was evaluated at different time intervals using the CyQUANT Assay. Data are the mean ± SD of three independent experiments, *P < 0.05 when comparing the specified groups by one-way ANOVA.

in the brain.

Author contributions

Conception and design: A.D., P.M., A.C., and R.B. Development of methodology: A.D., A.G., P.K.P., S.K.D.D., and F.N-A. Acquisition of data: A.D., P.K.P., S.K.D.D., T.K, F.N-A and H.R. Analysis and interpretation of data: A.D., P.K.P., H.R., A.C., P.M., and R.B. Writing and review of the manuscript: R.B., P.K.P., H.R., A.C., M.A., and P.M. Administrative, technical, or material support: P.M., A.C., M.A., and R.B. Study supervision: R.B. and P.M.

Data and materials availability

All data needed to evaluate the conclusions in the paper are present in the paper and/or the Supplementary Materials. Additional data related to this paper may be requested from the authors.

Declaration of competing interest

The authors declare that they havse no competing interests.

Data availability

Data will be made available on request.

Acknowledgements

Funding: This work was supported by NIH grants, 1R01HL120585 to (P.M. and R.B.) and by RF1AG072295 to A.C.

Appendix A. Supplementary data

Supplementary data to this article can be found online at https://doi.org/10.1016/j.redox.2023.102958.

References

[1] A. Verkhratsky, V. Untiet, C.R. Rose, Ionic signalling in astroglia beyond calcium, J. Physiol. 598 (9) (2020) 1655–1670.
[2] R. Siracusa, R. Fusco, S. Cuzzocrea, Astrocytes: role and functions in brain pathologies, Front. Pharmacol. 10 (2019) 1114.
[3] E.H. Joe, et al., Astrocytes, microglia, and Parkinson's disease, Exp Neurobiol 27 (2) (2018) 77–87.
[4] M.Y. Batiuk, et al., Identification of region-specific astrocyte subtypes at single cell resolution, Nat. Commun. 11 (1) (2020) 1220.
[5] A.M. Arranz, B. De Strooper, The role of astroglia in Alzheimer's disease: pathophysiology and clinical implications, Lancet Neurol. 18 (4) (2019) 406–414.
[6] T.I. Kam, et al., Microglia and astrocyte dysfunction in Parkinson's disease, Neurobiol. Dis. 144 (2020), 105028.
[7] B. Murphy, R. Bhattacharya, P. Mukherjee, Hydrogen sulfide signaling in mitochondria and disease, Faseb. J. 33 (12) (2019) 13098–13125.
[8] H. Zhao, et al., Brain 3-mercaptopyruvate sulfurtransferase (3MST): cellular localization and downregulation after acute stroke, PLoS One 8 (6) (2013), e67322.
[9] S. K.T.I.A.K.H.I.H.H.S.a.T, Development and aging expression of cystathionine-beta synthase in the temporal lobe and cerebellum of down syndrome patients, Neuroembryol. Aging 4 (2008).
[10] Y. Enokido, et al., Cystathionine beta-synthase, a key enzyme for homocysteine metabolism, is preferentially expressed in the radial glia/astrocyte lineage of developing mouse CNS, Faseb. J. 19 (13) (2005) 1854–1856.
[11] T. Panagaki, et al., Overproduction of hydrogen sulfide, generated by cystathionine beta-synthase, disrupts brain wave patterns and contributes to neurobehavioral dysfunction in a rat model of down syndrome, Redox Biol. 51 (2022), 102233.
[12] X. Shan, W.D. Kruger, Correction of disease-causing CBS mutations in yeast, Nat. Genet. 19 (1) (1998) 91–93.
[13] A. Dey, et al., Cystathione beta-synthase regulates HIF-1alpha stability through persulfidation of PHD2, Sci. Adv. 6 (27) (2020).
[14] B.A. Barshop, Homocystinuria and Hyperhomocysteinemia, 24 ed., Goldman's Cecil Medicine (Twenty Fourth Edition), 2012.
[15] J. Zivanovic, et al., Selective persulfide detection reveals evolutionarily conserved antiaging effects of S-sulfhydration, Cell Metabol. 30 (6) (2019) 1152–1170 e13.

[16] R. Tabassum, N.Y. Jeong, J. Jung, Therapeutic importance of hydrogen sulfide in age-associated neurodegenerative diseases, Neural Regen Res 15 (4) (2020) 653–662.
[17] D. Giovinazzo, et al., Hydrogen sulfide is neuroprotective in Alzheimer's disease by sulfhydrating GSK3beta and inhibiting Tau hyperphosphorylation, Proc. Natl. Acad. Sci. U. S. A. 118 (4) (2021).
[18] S. Prabhudesai, et al., Cystathionine beta-synthase is necessary for Axis development in vivo, Front. Cell Dev. Biol. 6 (2018) 14.
[19] G. Rao, et al., Cystathionine beta synthase regulates mitochondrial dynamics and function in endothelial cells, Faseb. J. 34 (7) (2020) 9372–9392.
[20] Y. Zhang, et al., Purification and characterization of progenitor and mature human astrocytes reveals transcriptional and functional differences with mouse, Neuron 89 (1) (2016) 37–53.
[21] J. Liu, et al., Quantitative chemoproteomics reveals O-GlcNAcylation of cystathionine gamma-lyase (CSE) represses trophoblast syncytialization, Cell Chem. Biol. 28 (6) (2021) 788–801 e5.
[22] D. Wang, et al., Inhibition of cystathionine beta-synthase promotes apoptosis and reduces cell proliferation in chronic myeloid leukemia, Signal Transduct. Targeted Ther. 6 (1) (2021) 52.
[23] A. Papapetropoulos, et al., Hydrogen sulfide is an endogenous stimulator of angiogenesis, Proc. Natl. Acad. Sci. U. S. A. 106 (51) (2009) 21972–21977.
[24] J.B. Owen, D.A. Butterfield, Measurement of oxidized/reduced glutathione ratio, Methods Mol. Biol. 648 (2010) 269–277.
[25] Y. Zhang, et al., An RNA-sequencing transcriptome and splicing database of glia, neurons, and vascular cells of the cerebral cortex, J. Neurosci. 34 (36) (2014) 11929–11947.
[26] M. Ximerakis, et al., Single-cell transcriptomic profiling of the aging mouse brain, Nat. Neurosci. 22 (10) (2019) 1696–1708.
[27] J.L. Gollihue, C.M. Norris, Astrocyte mitochondria: central players and potential therapeutic targets for neurodegenerative diseases and injury, Ageing Res. Rev. 59 (2020), 101039.
[28] J. Qiao, et al., Regulation of platelet activation and thrombus formation by reactive oxygen species, Redox Biol. 14 (2018) 126–130.
[29] S. Saha, et al., Cystathionine beta-synthase regulates endothelial function via protein S-sulfhydration, Faseb. J. 30 (1) (2016) 441–456.
[30] X. Chen, C. Guo, J. Kong, Oxidative stress in neurodegenerative diseases, Neural Regen Res 7 (5) (2012) 376–385.
[31] F. Comas, et al., Permanent cystathionine-beta-Synthase gene knockdown promotes inflammation and oxidative stress in immortalized human adipose-derived mesenchymal stem cells, enhancing their adipogenic capacity, Redox Biol. 42 (2021), 101668.
[32] I. Ishii, et al., Murine cystathionine gamma-lyase: complete cDNA and genomic sequences, promoter activity, tissue distribution and developmental expression, Biochem. J. 381 (Pt 1) (2004) 113–123.
[33] H.D.E. Booth, W.D. Hirst, R. Wade-Martins, The role of astrocyte dysfunction in Parkinson's disease pathogenesis, Trends Neurosci. 40 (6) (2017) 358–370.
[34] B.S. Khakh, et al., Unravelling and exploiting astrocyte dysfunction in huntington's disease, Trends Neurosci. 40 (7) (2017) 422–437.
[35] K. Modis, et al., S-Sulfhydration of ATP synthase by hydrogen sulfide stimulates mitochondrial bioenergetics, Pharmacol. Res. 113 (Pt A) (2016) 116–124.
[36] A.K. Mustafa, et al., H2S signals through protein S-sulfhydration, Sci. Signal. 2 (96) (2009) ra72.
[37] G. Yang, et al., Hydrogen sulfide protects against cellular senescence via S-sulfhydration of Keap1 and activation of Nrf2, Antioxidants Redox Signal. 18 (15) (2013) 1906–1919.
[38] K.N. Maclean, E. Kraus, J.P. Kraus, The dominant role of Sp1 in regulating the cystathionine beta-synthase -1a and -1b promoters facilitates potential tissue-specific regulation by Kruppel-like factors, J. Biol. Chem. 279 (10) (2004) 8558–8566.
[39] Y. Ge, et al., Transcriptional regulation of the human cystathionine beta-synthase -1b basal promoter: synergistic transactivation by transcription factors NF-Y and Sp1/Sp3, Biochem. J. 357 (Pt 1) (2001) 97–105.
[40] A. Prudova, et al., S-adenosylmethionine stabilizes cystathionine beta-synthase and modulates redox capacity, Proc. Natl. Acad. Sci. U. S. A. 103 (17) (2006) 6489–6494.
[41] S. Kreuz, W. Fischle, Oxidative stress signaling to chromatin in health and disease, Epigenomics 8 (6) (2016) 843–862.
[42] E. Disbrow, et al., Plasma hydrogen sulfide: a biomarker of Alzheimer's disease and related dementias, Alzheimers Dement 17 (8) (2021) 1391–1402.
[43] T.H. Reekes, et al., Elevated plasma sulfides are associated with cognitive dysfunction and brain atrophy in human Alzheimer's disease and related dementias, Redox Biol. 62 (2023), 102633.
[44] P.K. Chakraborty, et al., Cystathionine beta-synthase regulates mitochondrial morphogenesis in ovarian cancer, Faseb. J. 32 (8) (2018) 4145–4157.